[C II] and [N II] Observations of Ionized Gas at the Edge of the Central Molecular Zone*

Bill Langer (JPL-Caltech)

January 21, 2015

Collaborators: P. F. Goldsmith[1], J. L. Pineda[1], M. A. Requena-Torres[2], T. Velusamy[1], H. Wiesemeyer[2]

1. JPL-Caltech, Pasadena, CA, USA
2. MPIFR, Bonn, Germany

* A&A (2015) in press.

The Superlative Central Molecular Zone

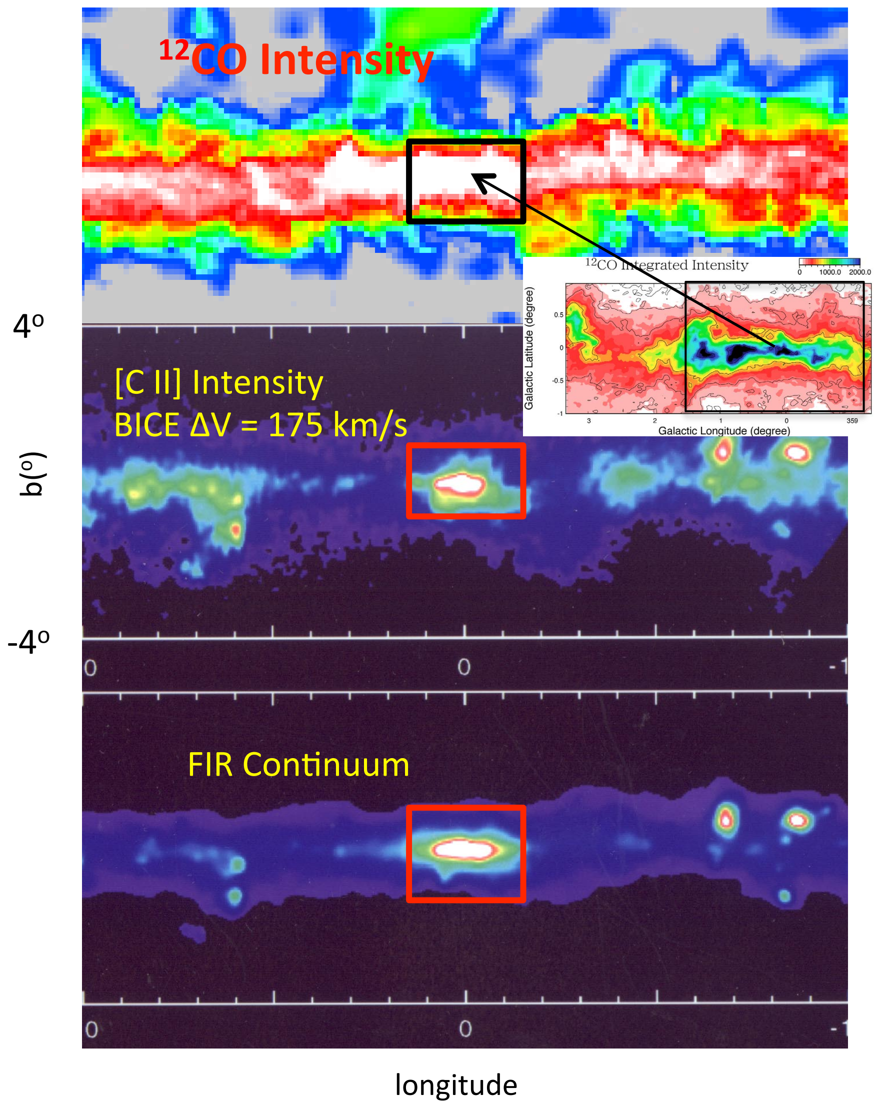

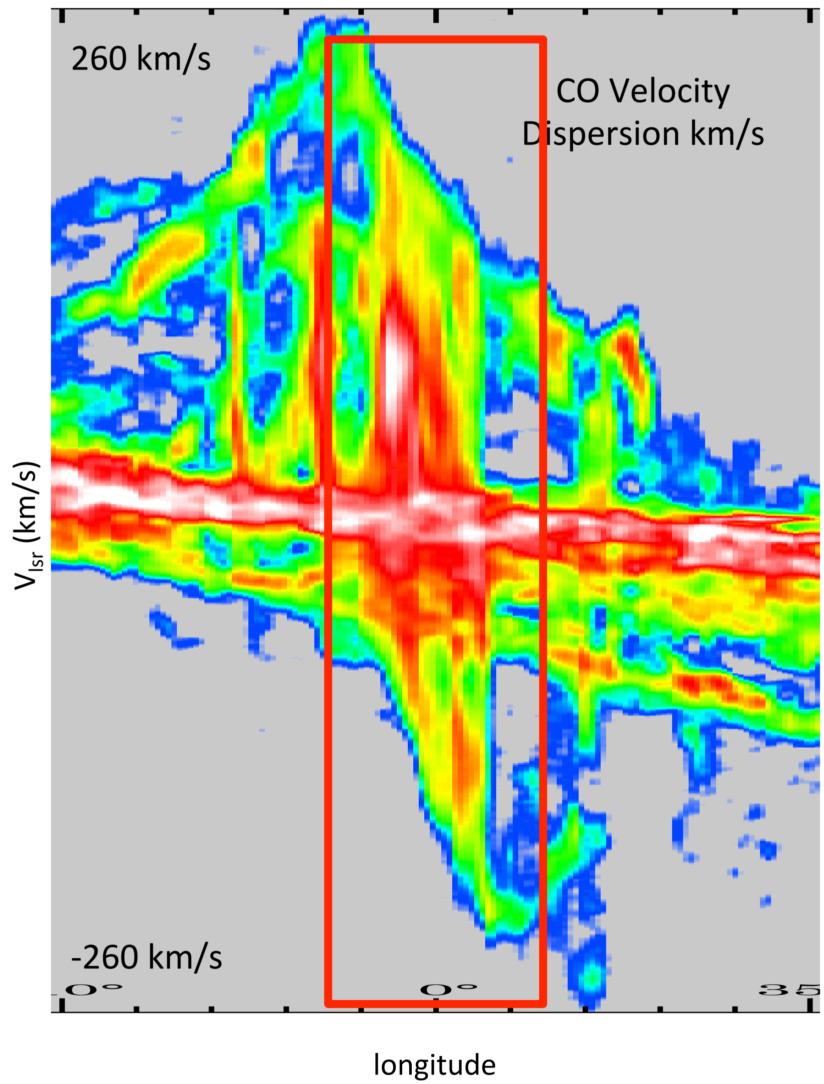

CO from Dame et al. (2001) & Nobayama CO survey Oka et al (1998); [C II] BICE survey Nakagawa et al. (1998)

Outline

- Overview of CMZ
- [N II] and [C II]
- Electron abundance
- Results
- Ionization Sources
- Conclusion

Special thanks to: Rolf Güsten and Göran Sandell for their effort during the GREAT SOFIA observing runs. Erick Young for his support in scheduling decisions. David Teyssier of HSC for his advice with the HIPE pipeline data reduction.

Central Molecular Zone (CMZ)

- CMZ ≈400 pc X 80 pc around the Galactic Center
- Giant Molecular Clouds (GMCs) ≈few$\times10^7$ $M_\odot$
- GMCs: $n(H_2)$ > 10 X disk
- T_{kin} ≈ 40 – 200K vs 10 - 35K
- ΔV ≈ 20 km/s vs 3-4 in disk
- H ≈ (2 – 10)x10^5 $M_\odot$

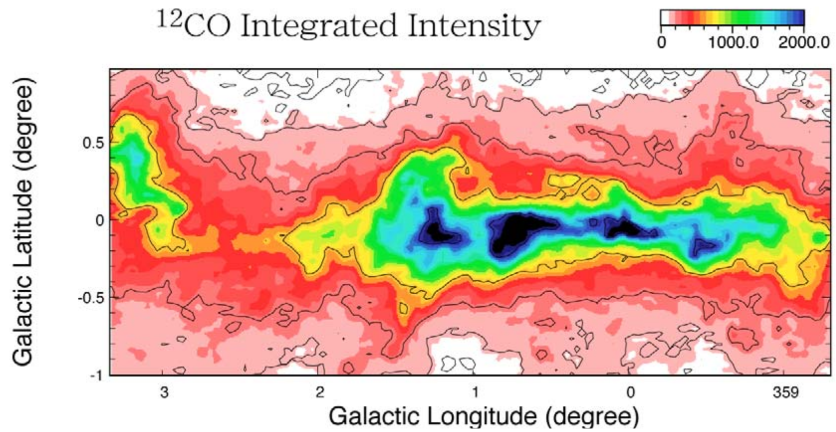

Moriguchi 2005

- H^+ ≈ (6–10)x10^5 $M_\odot$: WIM (H^+), HIM(H^+,He^+)
- Enhanced energy environment: HII regions, accreting black holes, X-rays, cosmic rays, supernova, turbulence.

See reviews by Morris & Serabyn (1996) ARA&A and Ferriere et al. (2007) A&A

Ionized Gas in the Galaxy

- Ionized gas is an important component of the ISM
- It occupies most of the volume
- Couples gas to magnetic fields
- Physical state of the ionized gas is a result of sources of ionization and heating (star formation rate, accreting black holes, cosmic rays, etc.)
- Boundary pressure for the HI clouds and GMCs

Distribution of CMZ Gas - Molecular

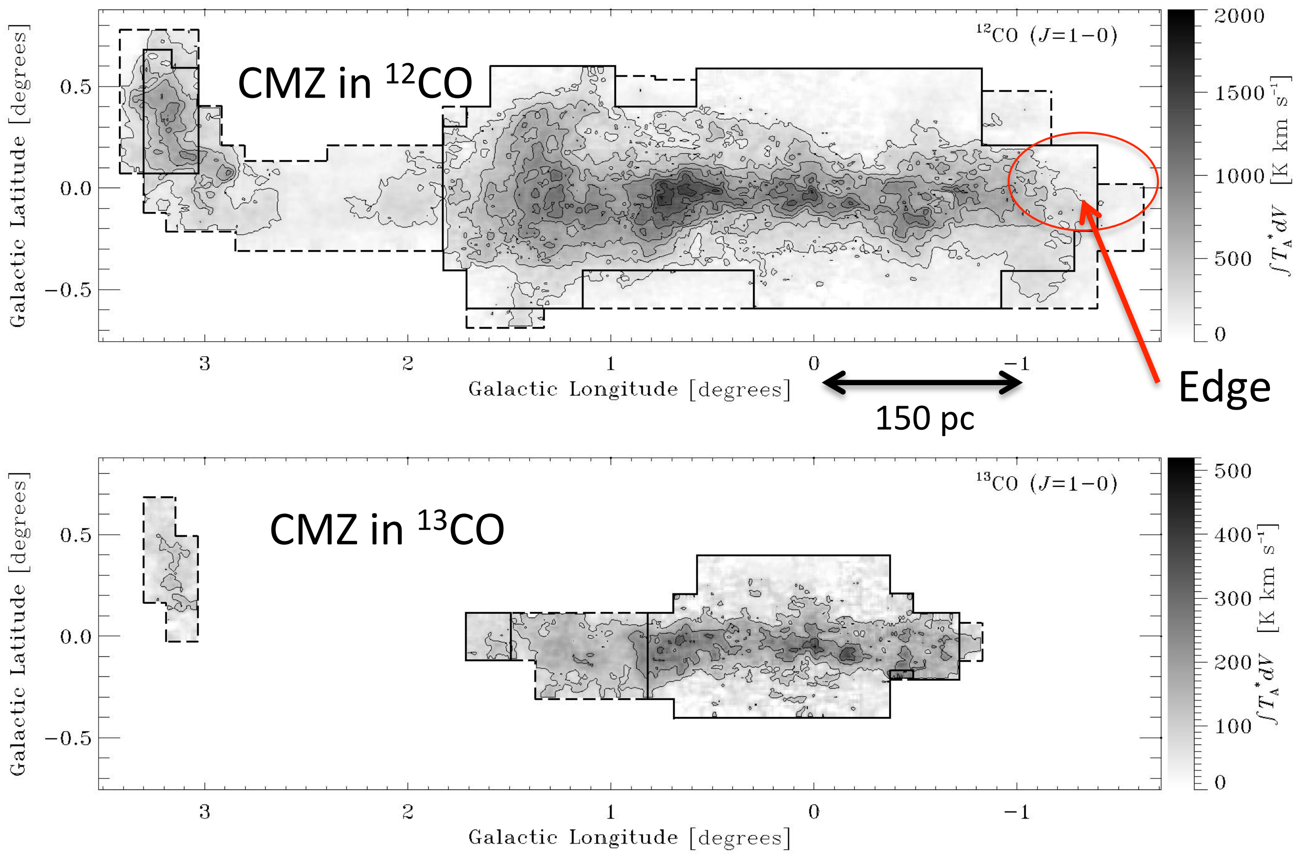

FIG. 2.—Maps of the ^{12}CO $J = 1$–0 and ^{13}CO $J = 1$–0 line emission integrated over the velocity range $V_{LSR} = -220$ to $+220$ km s^{-1}. Contours drawn at every 200 K km s^{-1} for ^{12}CO and at every 100 K km s^{-1} for ^{13}CO. Mapping areas are indicated by solid lines (four beams) and dashed lines (t beams).

Nobayama Telescope (Oka et al. 1998)

Measuring Electron Abundance (Examples)

- Radio-Wave dispersion against embedded (pulsar) or background (extragalactic) sources
- Radio continuum from thermal free-free emission
- Radio recombination lines, e.g. H110α.
- X-ray lines – Fe ions (Fe XXV) probes very hot gas
- Visual – e.g. Hα λ6563
  - Wisconsin H Alpha Mapper (WHAM)
- Far IR fine-structure lines, e.g. [C II], [N II], [O III]
  - [C II] at 1.90 THz (158 μm) and [N II] at 1.46 THz (205 μm)
  - Advantage of high spectral resolution with heterodyne receivers

Radio Continuum and Recombination

- Mezger & Pauls (1979) derived n(e) distribution in CMZ using radio continuum (thermal free-free) and recombination lines
- Modeled WIM as two oblate spheroids
  - $(225\ \mathrm{pc})^2 \times 90$ pc with n(e) ≈ 8 cm^{-3} & T(e) ≈ 5000 K, $M(H^+) \approx 4.7\times10^5\ M_\odot$
  - $(95\ \mathrm{pc})^2 \times 55$ pc with n(e) ≈ 18 cm^{-3} & T(e) ≈ 5000 K, $M(H^+) \approx 1.2\times10^5\ M_\odot$
  - Total inner n(e) ≈ 26 cm^{-3} & $M(H^+) \approx 5.9\times10^5\ M_\odot$
- n(e) is very high compared to n(e) ≈ 0.01 for Disk WIM

n(e) from Radio Dispersion

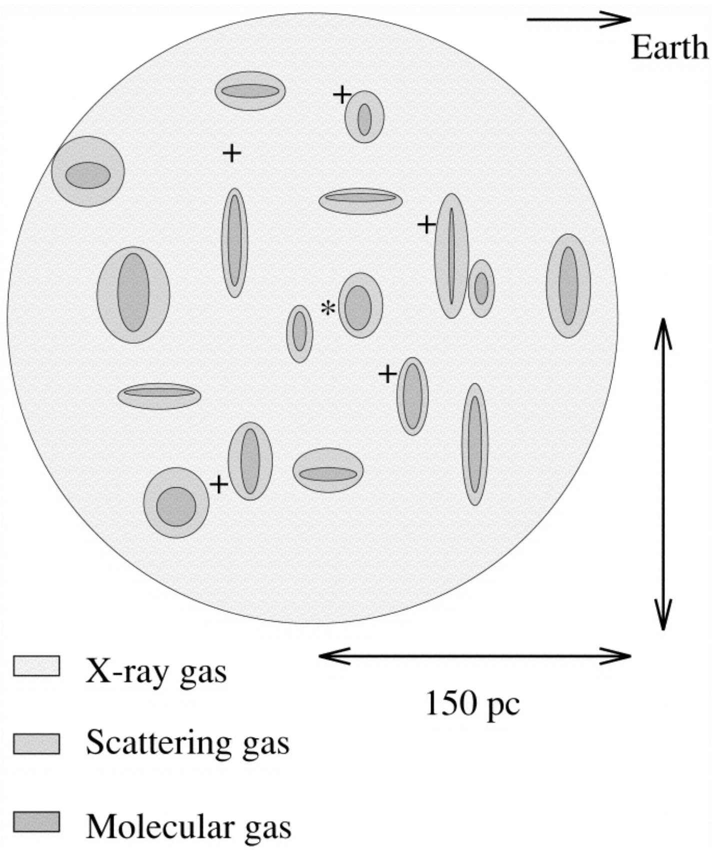

Lazio & Cordes (1998) conclude dispersion is due to scattering off either:

a. Photoionized skins of molecular clouds with $T(e) \approx 10^4$ K and $n(e) > 10^3$ cm^{-3} , or
b. Interface between molecular clouds and the hot ambient gas with $T(e) \approx 10^{5-6}$ K and $n(e) \approx 5 – 50$ cm^{-3}

Roy (2013) observed 62 compact extragalactic sources towards CMZ

a. Scattering medium is patchy on scales of ≈10’ (25 pc) with $n(e) \approx 10$ cm^{-3}
b. Ionized interfaces with dense GMCs are likely source of scattering.

see also review by Ferriere et al. (2007)

HIM: X-Ray Observations

Iron distribution

Suzaku image

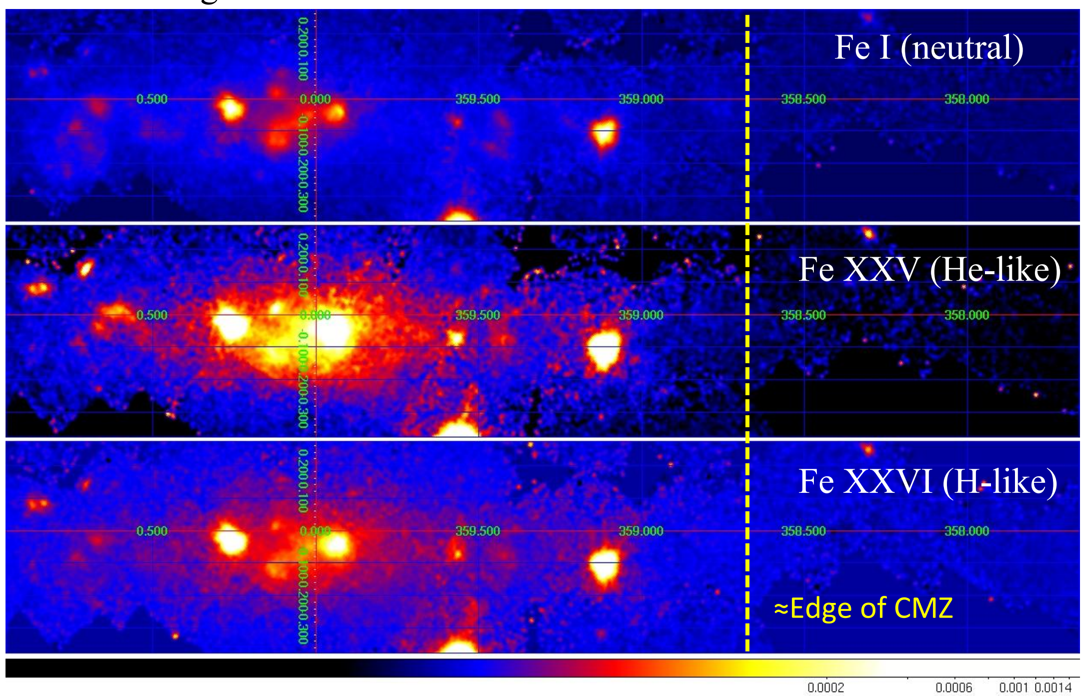

- X-ray thermal emission at 0.5 to 2 keV (ROSAT) is enhanced towards CMZ - Hot Ionized Medium (HIM)
- Hard X-ray emission from Fe XXV and Fe XXVI (Koyama et al. 1996): kT> several keV, n(e) ≈ 0.03 cm^{-3} , $M(H^{+}) \approx 10^{5}\ M_{\odot}$

n(e) from [N II] and [C II]

- Use [N II] and [C II] far-infrared lines to probe the electron density and ionization in the CMZ
- ADVANTAGE: High spectral resolution identifies components and probes physical properties
- [C II] traces all ionized regions as I.P. = 11.1 eV
- [N II] traces more highly ionized gas: I.P. = 14.53 eV
- *Herschel* HIFI OTF [C II] strip maps → morphology
- *SOFIA* GREAT [C II] and [N II] pointed observations along a strip across the edge of the CMZ → n(e)

Edge of the CMZ in CO and [C II]

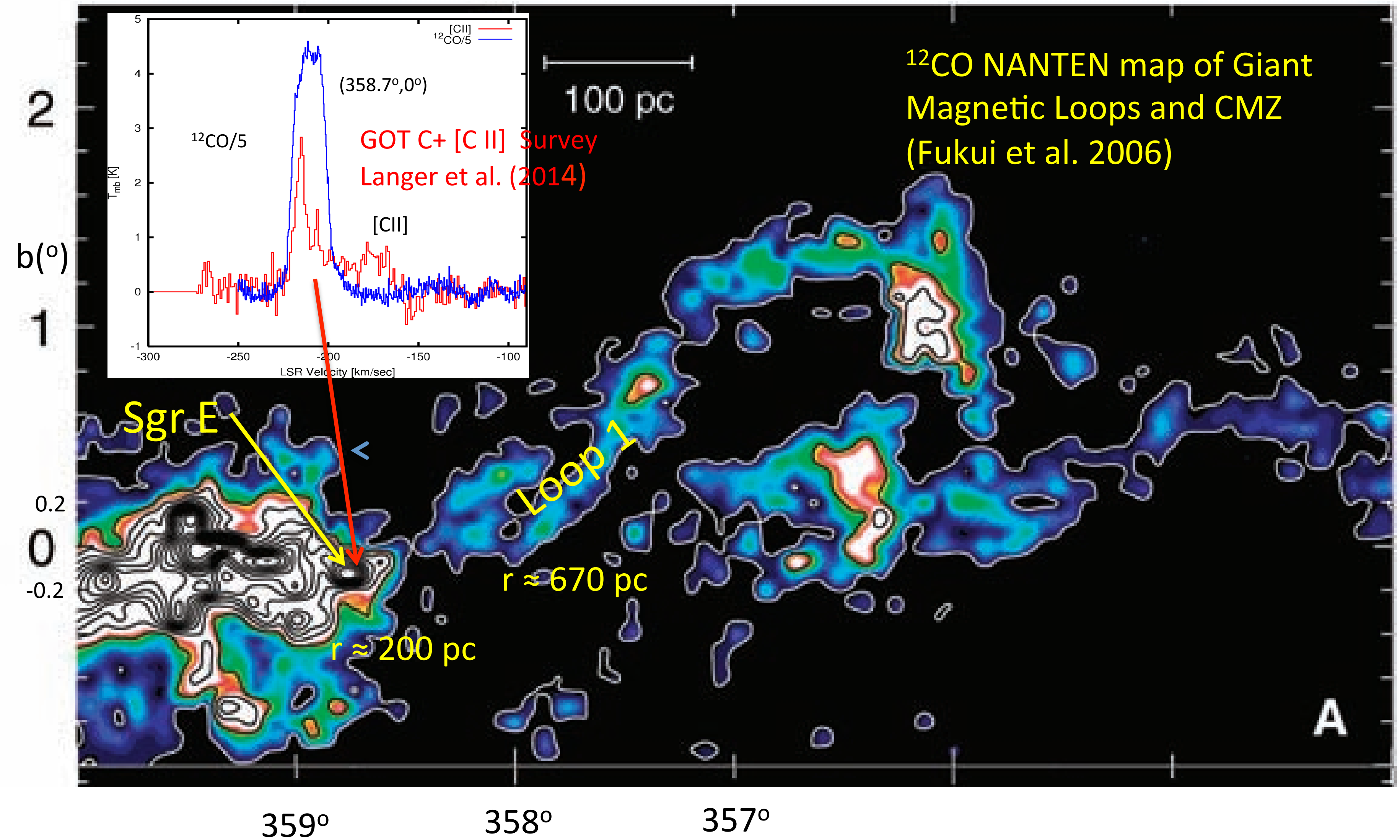

^{12}CO map from Oka et al. 1998

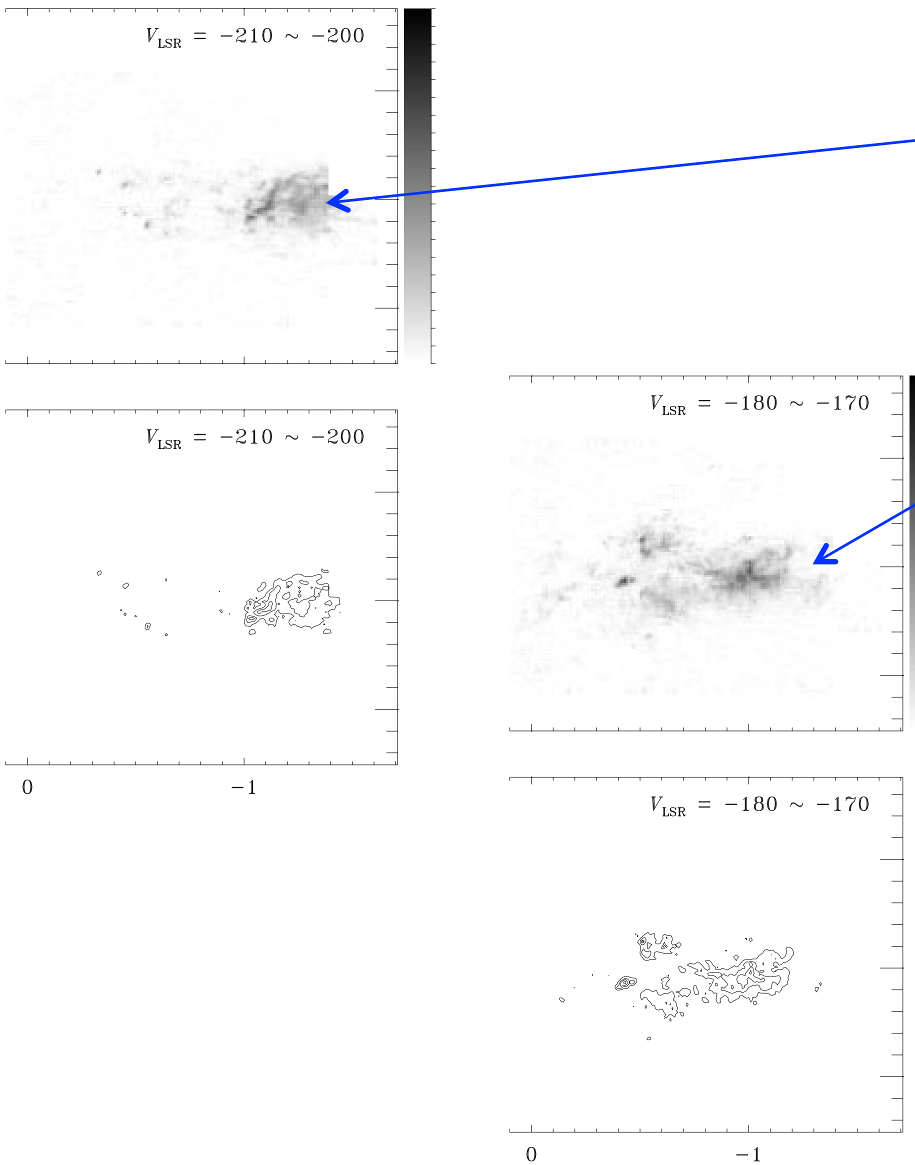

Herschel HIFI [C II] and Mopra ^{12}CO

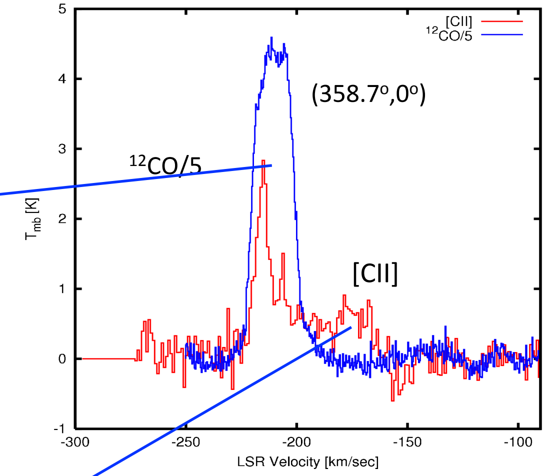

[C II] probes the ionized edge of these GMCs

CMZ [C II] OTF Map

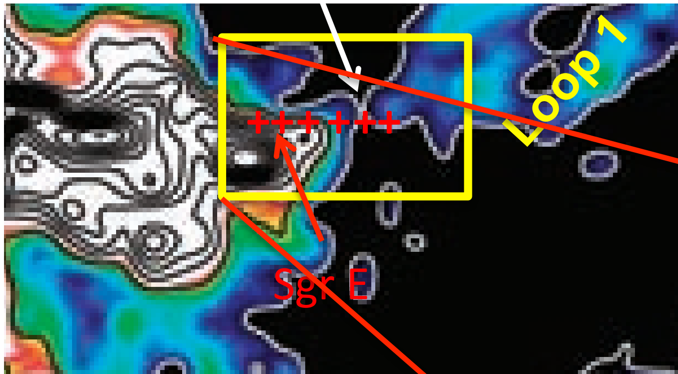

HIFI OTF

GREAT +

[C II] strongest at CO boundary
– limb brightening

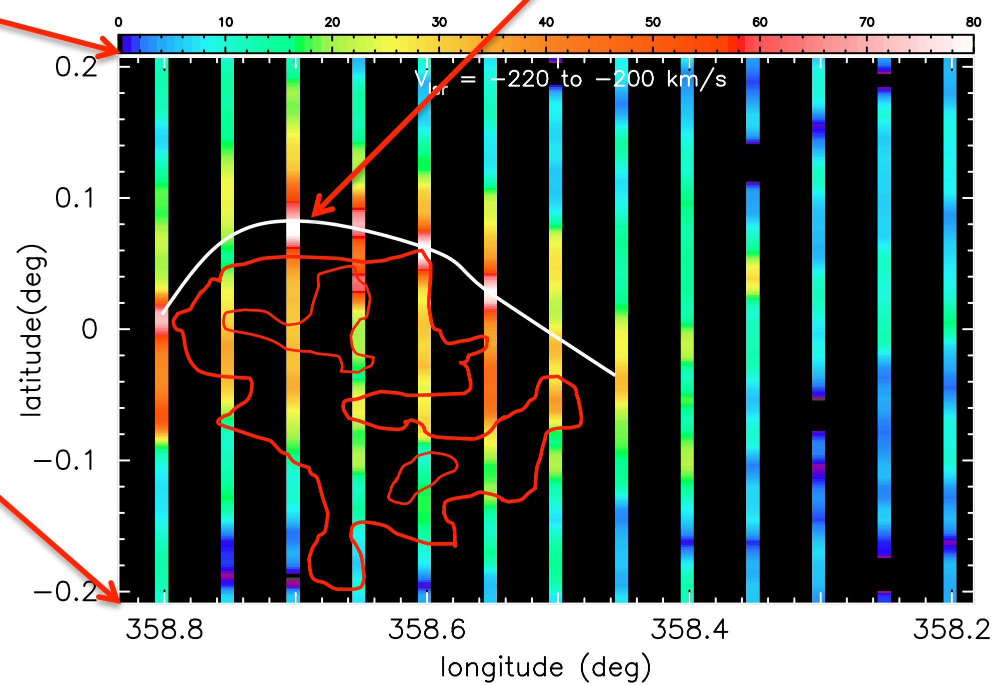

HIFI OTF [CII] intensity (color)
Contours CO -210 to -220 km/s (Oka 1998)

GREAT [C II] & [N II] along $b=0^o$

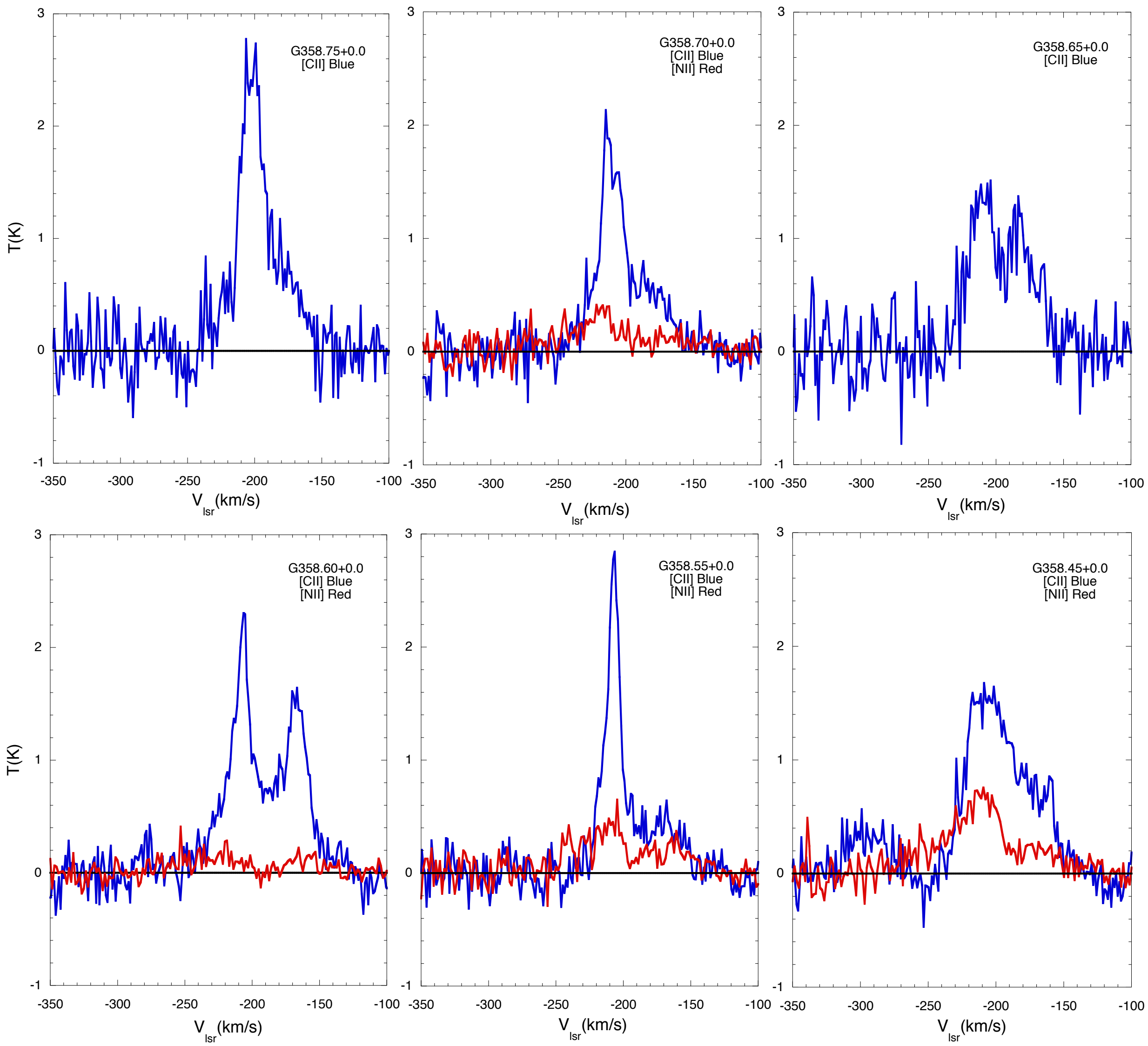

[C II] detected at all 6 LOS – 2 components

[N II] detected at 4 LOS where S/N was best – 2 components

Components

V_{lsr}(km/s)	ΔV(km/s)
-207	≈25-30
-174	≈25-30

GREAT [CII] & [NII] – Data Reduction Issues

Atmospheric H_2O line in [C II] band
Emission in reference off position

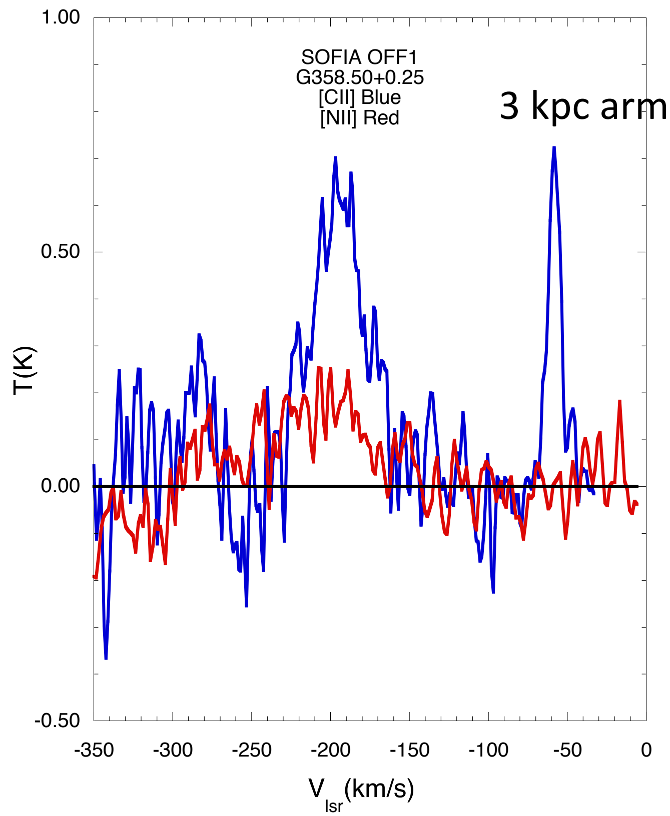

Emission in OFF1

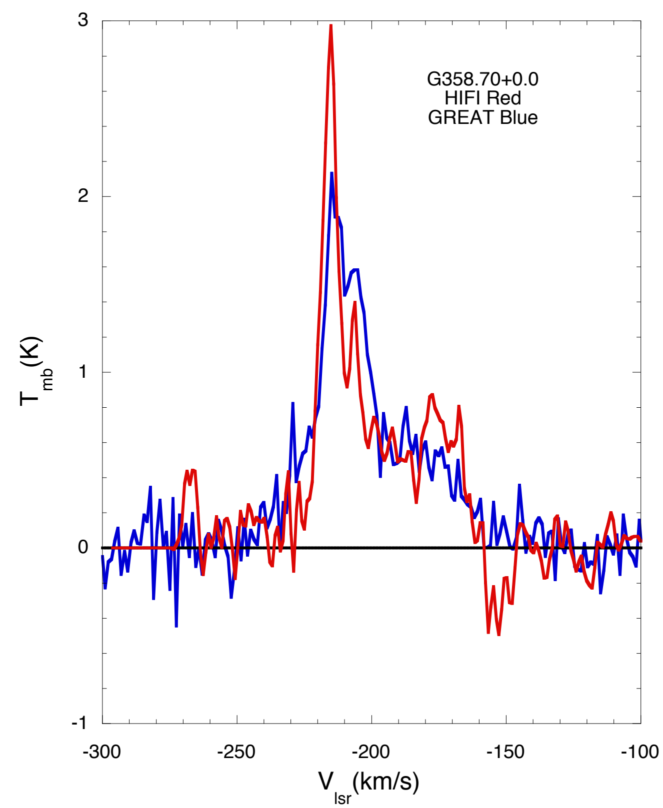

[C II] GREAT vs GOT C+

CO and HI (b=0°)

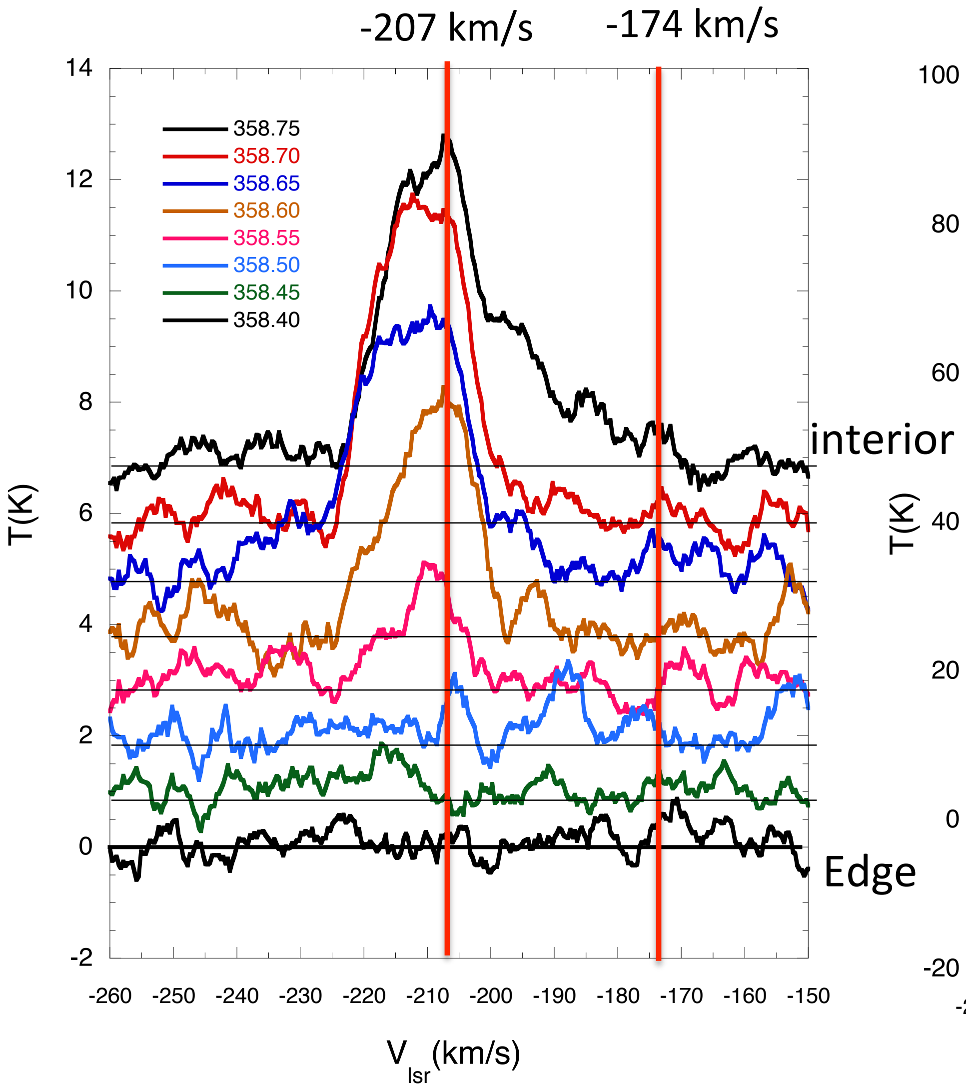

ThrUUMS (Three-mm Ultimate Mopra Milky Way Survey)

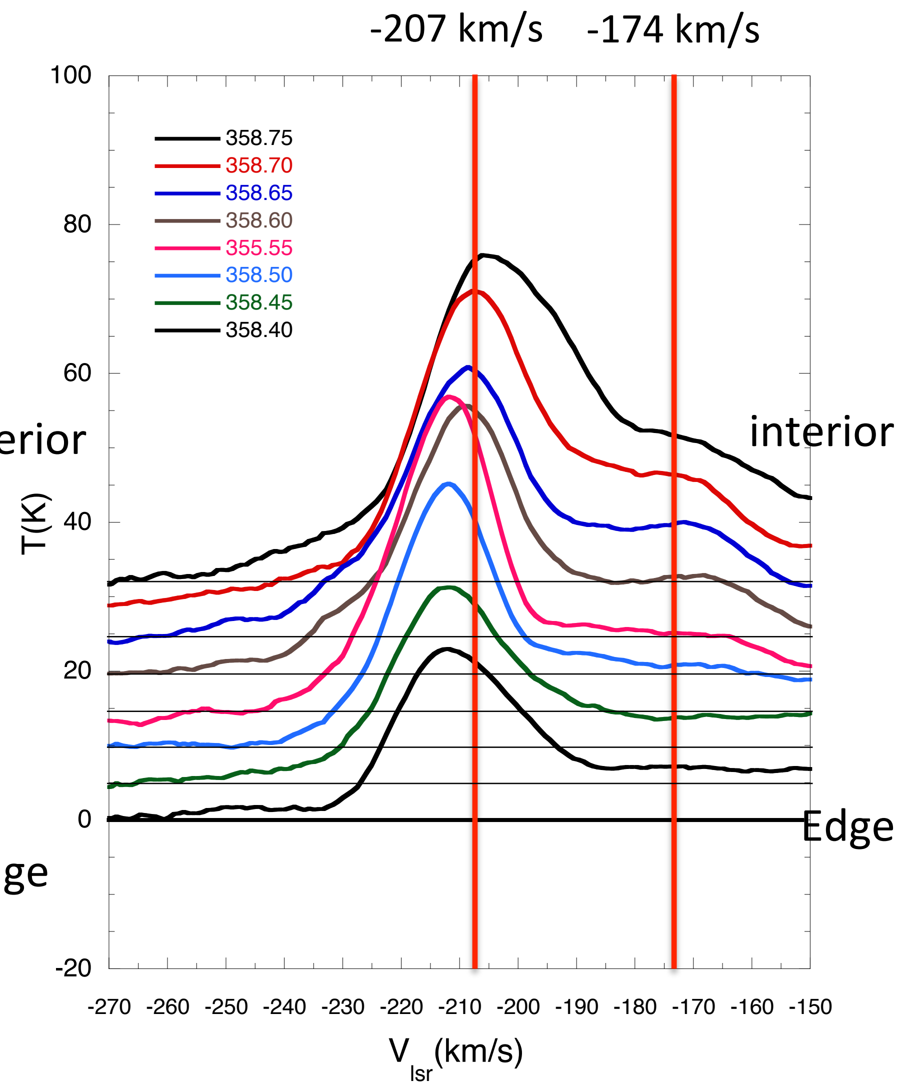

HI Survey (McClure-Griffiths et al. 2012

Line Parameters

Table 1. Integrated line intensities

LOS	I([C II])[a,b]	I([N II])[c]	I(CO)	I(H I)
V_{lsr} = -207 km s^{-1}				
358.45+0.0	63.4	26.4	6.7	1047
358.55+0.0	45.4	15.4	26.6	1904
358.60+0.0	47.6	7.1	60.6	2189
358.65+0.0	38.6	-	101.9	2539
358.70+0.0	45.4	12.4	98.9	2923
358.75+0.0	57.4	-	110.5	3235
V_{lsr} = -174 km s^{-1}				
358.45+0.0	21.1	8.2	-	730
358.55+0.0	12.2	8.8	-	1212
358.60+0.0	43.0	3.7	-	1544
358.65+0.0	25.5	-	-	1855
358.70+0.0	15.3	5.3	-	2177
358.75+0.0	21.8	-	9.8	2522

a) Integrated intensities are in units of K km s^{-1}. We only report detections with a SNR ≥ 3, see text. b) Typical rms noise in the [C II] integrated intensity is ~1.4 K km s^{-1}. c) Typical rms noise in the [N II] ntegrated intensity is ~1.3 K km s^{-1}.

SNR ranges from 4 to 20 for I(NII) and 8 to 45 for I(CII)

ΔV of order 25 to 35 km/s

n(e) from [N II] – 2 levels

Electron collisions dominate excitation.
Solve the population of the 3 levels assuming τ << 1.

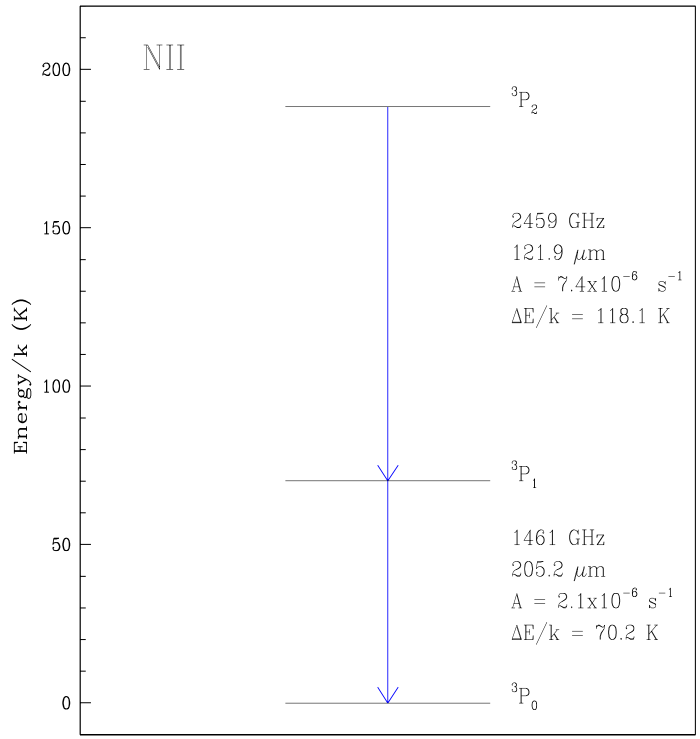

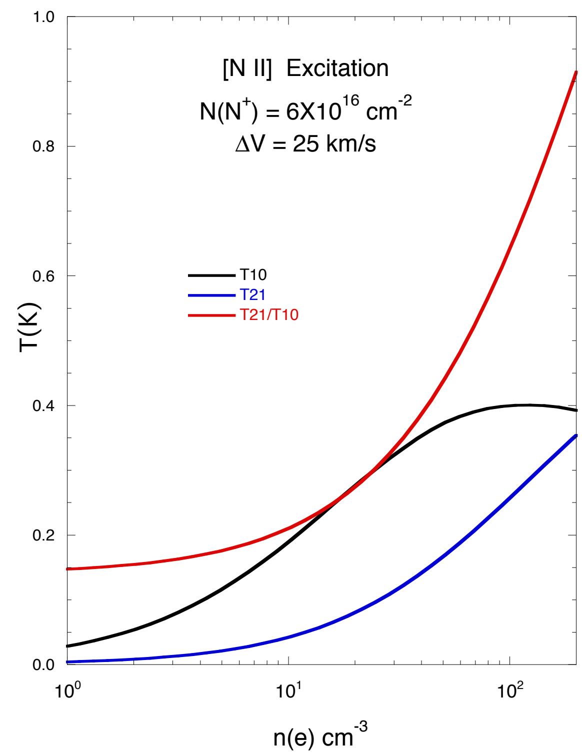

n(e) sensitive to ratio of 122μ to 205μ line only for n(e) > 10 cm^{-3}
1-0 line difficult to detect for n(e) < few cm^{-3} & 2-1 is even harder.

n(e) from [N II] – 1 transition (1/2)

$$\tau << 1$$

$$I_{10}([NII]) = T_{10}(K)\Delta V$$

$$= \frac{hc^3}{8\pi\nu_{10}^2} A_{10} f_1(N^+) N(N^+) \text{ cm}^{-2}$$

Where f_1 is the fractional population of $^2P_1$ state of N^+ and is a function of n(e)

With only one line need to estimate $N(N^+)$

Assume uniform conditions: $N(N^+) = n(N^+)L$ cm^{-2}

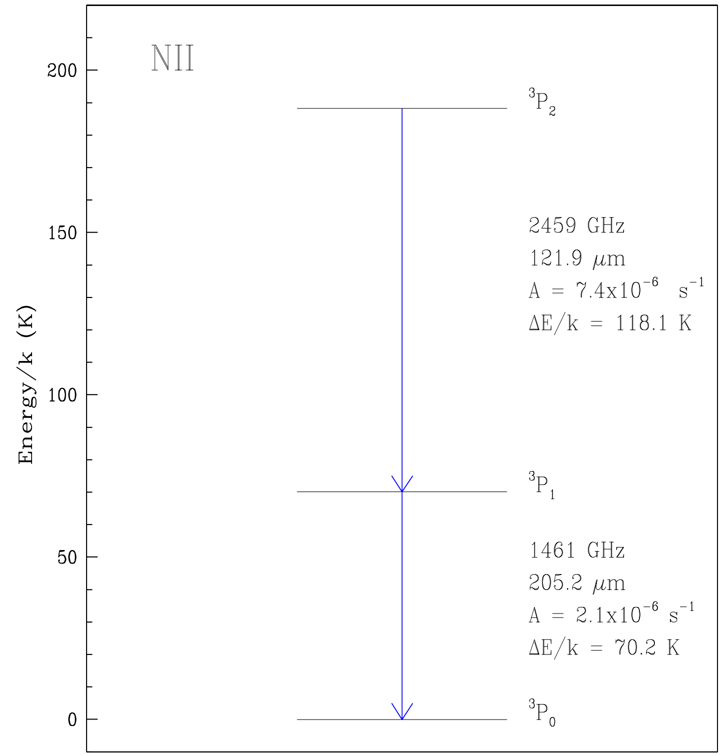

$$I_{10}([NII]) \approx 5 \times 10^{-16} (n(N^+)L) f_1 \text{ cm}^{-2}$$

n(e) from [N II] – 1 transition (2/2)

$$n(N^+) = x(N^+)n(H^+)$$

$$n(H^+) \doteq n(e)$$

$$I_{10}([NII]) \approx 0.16 x_{-4}(N^+) L_{pc} n(e) f_1(N^+)\ \mathrm{cm}^{-2}$$

$f_1(N^+)$ is independent of $N(N^+)$ if $\tau \ll 1$

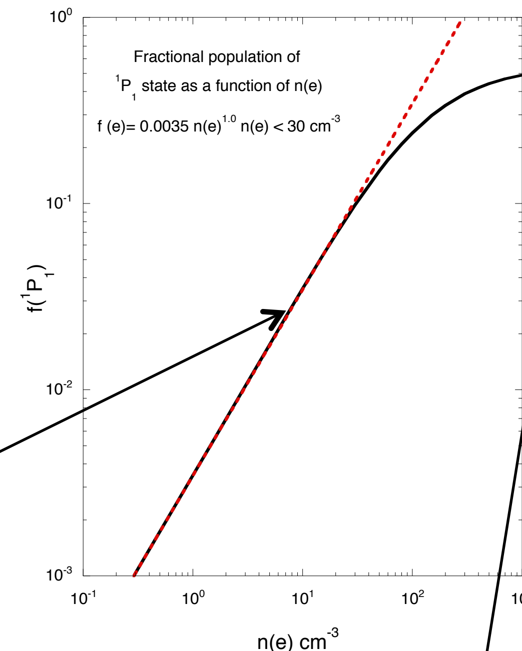

$n(e) \ll n_{cr}(e)$: $f_1 \propto n(e)$

$$n(e) \simeq \left[\frac{6.4 I([NII]) n_{cr}(e)}{L_{pc} x_{-4}(N^+)}\right]^{0.5}$$

$n(e) \gg n_{cr}(e)$: f_1 -> const

$$n(e) \propto \left[\frac{I([NII])}{L_{pc} x_{-4}(N^+)}\right]^{\simeq 1}$$

Model Parameters

- -207 km/s component
  - [C II] limb brightened
  - Ionized layer ≈ 15 pc thick
  - $X(N^+) \approx 1.6X10^{-4}$ (3xSolar)
  - Solve n(e) for each I([NII])
  - Not very sensitive to $x(N^+)$ & L_{pc}

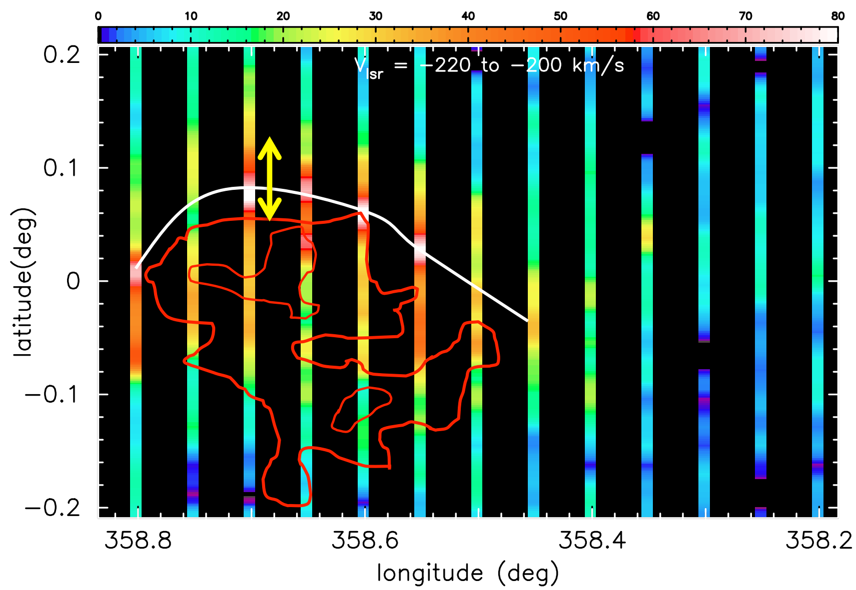

- -174 km/s component
  - OTF HIFI map of this weaker [C II] component is not good enough to reveal morphology of emission region
  - Assume same parameters as -207 km/s component

Electron and Column Densities

Table 2. Electron density and nitrogen column density

$V_{lsr}{}^{a}$ = LOS	-207 $n(e)^{b}$	-207 $N(N^+)^{c}$	-207 $N(H^+)$	-174 $n(e)^{d}$	-174 $N(N^+)$	-174 $N(H^+)$
358.45[e]	20.7	1.5e17	9.6e20	9.9	7.5e16	4.6e20
358.55	14.6	1.1e17	6.8e20	10.4	7.9e16	4.8e20
358.60	9.1	6.9e16	4.2e20	6.3	4.8e16	2.9e20
358.65	-	-	-	-	-	-
358.70	12.8	9.7e16	5.9e20	7.7	5.9e16	3.6e20
358.75	-	-	-	-	-	-
Average	14.3	1.1e17	6.6e20	8.6	6.5e16	4.0e20

a) In km s^{-1}. b) Densities in cm^{-3}. c) Column densities in cm^{-2}. d) In cm^{-3}. e) All LOS are along b =0°.

Table 3. C^+ column densities and intensities

LOS[a]	$N(C^+)^{b}$	$I_{H^+}([C\,II])^{c}$	$I_{H_2}([C\,II])$	$N_{H_2}(C^+)$	$N_{C^+}(H_2)^{f}$
-207[d]					
358.45	4.9e17	64.1	-0.7	-	-
358.55	3.5e17	38.5	7.0	4.2e17	8.2e20
358.60	2.2e17	18.3	29.3	1.8e18	3.5e21
358.65	-	-	-	-	-
358.70	3.0e17	31.3	14.1	8.6e17	1.7e21
358.75	-	-	-	-	-
Average	3.4e17	38.1	16.8[e]	1.0e18	2.0e21
-174[d]					
358.45	2.4e17	21.1	0.1	3.3e15	6.4e18
358.55	2.5e17	22.6	-10.4	-	-
358.60	1.5e17	9.9	33.1	2.0e18	3.9e21
358.65	-	-	-	-	-
358.70	1.8e17	13.4	1.3	8.2e16	1.6e20
358.75	-	-	-	-	-
Average	2.0e17	16.9	11.5[e]	7.0e17	1.4e21

a) All LOS are at b =0°. b) Column density in cm^{-2}. c) Intensity of [C II] in the [N II] emission region in K km s^{-1}. d) V_{lsr} in km s^{-1}. e) Negative intensities are not included. f) Assumes T_k=100K and $n(H_2)$ = 300 cm^{-3}.

- V_{lsr} = -207 km/s component
  - n(e) = 9 - 21 cm^{-3}
  - $N(N^+)$ =(7 – 15)X10^{16} cm^{-2}
- V_{lsr} = -174 km/s component
  - n(e) = 6 - 10 cm^{-3}
  - $N(N^+)$ =(5 – 8)X10^{16} cm^{-2}

Results

- [N II] and [C II] Detections provide evidence of hot highly ionized gas with n(e) ≈ 5 to 25 cm^{-3} in a thick layer surrounding GMCs in the Sgr E region.

- n(e) consistent with suggestions by Lazio & Cordes (1998) and Roy (2013) that dispersion of radio waves in the CMZ is primarily by scattering at the interface of clouds with a dense hot ionized medium

Ionization Sources (1/3)

- Electron collisional ionization
- Cosmic ray ionization
- EUV photoionization
- X-ray photoionization
- Proton charge exchange
  - $UV + H \rightarrow H^+ + e$
  - $H^+ + N \leftrightarrow H + N^+$ ($\Delta E = 0.94$ eV $\approx 11,000$ K)

Ionization Sources (2/3)

- ~~Electron collisional ionization requires very high kinetic temperatures as I.P. = 14.53 eV~~
- ~~Cosmic ray ionization need 10^{-12} s^{-1} –~~
  - ~~observations of H_3^+ in CMZ (Goto et al. 2014) suggest rate is too low by orders of magnitude~~

Ionization Sources (3/3)

- EUV photoionization: Need EUV flux 6×10^6 photons/cm^2/s – source massive star formation (O & B)
- X-ray photoionization of nitrogen & carbon about 10^3 larger than corresponding H photoionization
  - Sources: diffuse X-rays, stellar sources, accreting black holes (stellar and massive)
- Charge exchange: $H^+ + N \leftrightarrow H + N^+$ ($\Delta E = 0.94$ eV)
  - H ionized by UV
  - $T_{kin} \approx 6{,}000$ K to 15,000 K depending on theoretical cross sections (see Lin et al. 2005; Langer et al. 2015)
  - Heating source: Shocks? Turbulent dissipation? EUV & X-rays?

Compact and Diffuse HII Sources

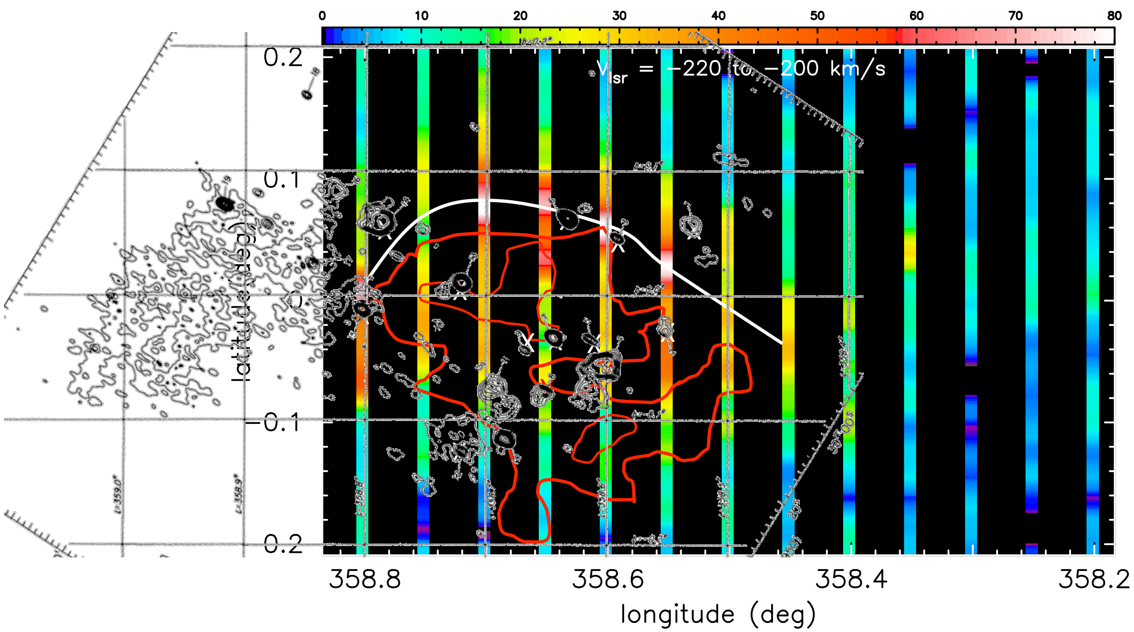

- Sgr E is an active star-forming HII region associated with a GMC
- VLA radio continuum map of Sgr E region (Liszt 1992)
  - 18 compact HII sources
    - $n(e) \approx$ few$\times 10^2$ cm^{-3}
    - ionizing stars are likely B0 or brighter
  - diffuse emission *l* = 358.8° to 358.95°

Edge of CMZ in IR

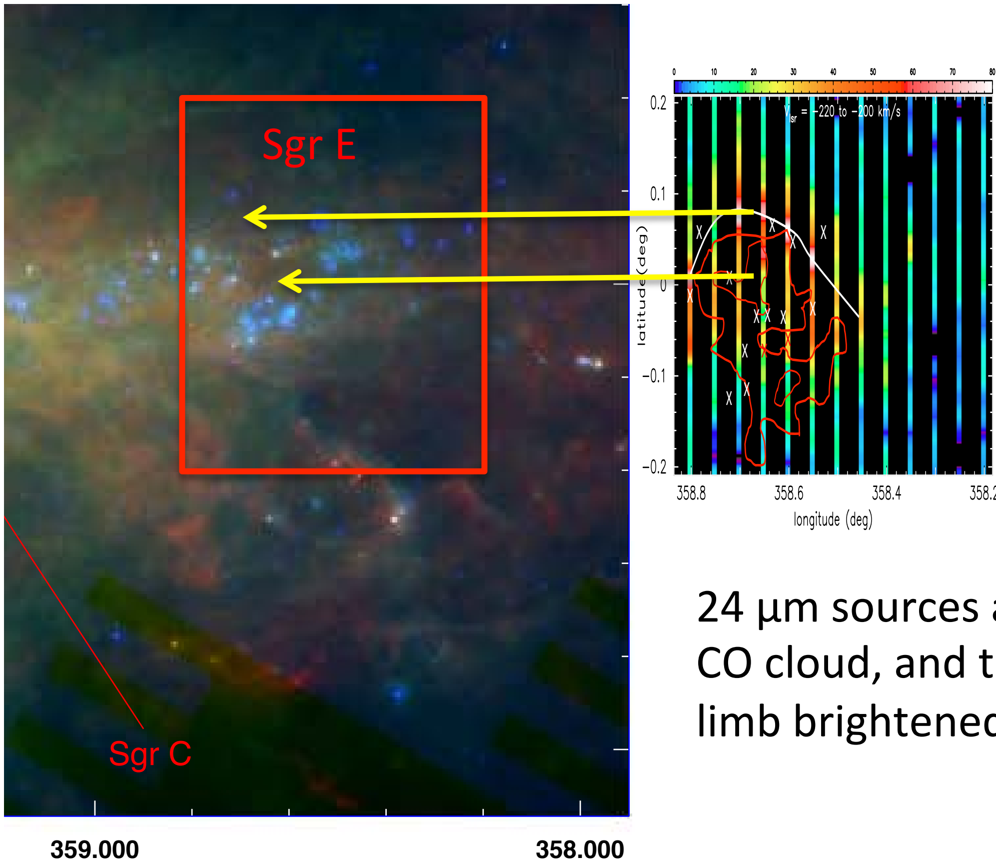

Spitzer 24 μm (blue)
Herschel 70 μm (green)
Herschel 500 μm (red)
from Molinari et al. (2014)

24 μm sources associated with the CO cloud, and the edge of the [C II] limb brightened arc

Hot Gas in the CMZ Traced by X-rays

Iron distribution

Suzaku image

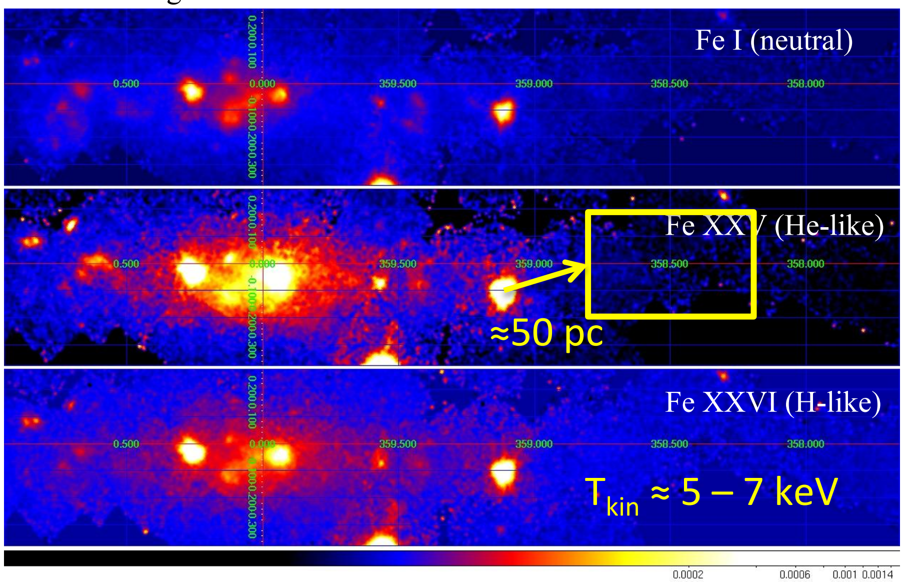

Suzaku X-ray satellite (Koyama et al. 2007; from Matsumoto presentation)

Diffuse and discrete (> 9000) X-Ray sources detected by *Chandra* (Wang et al. 2002; Muno et al. 2009)

Red: 1 – 3 keV

Green: 3 – 5 keV

Blue: 5 – 8 keV

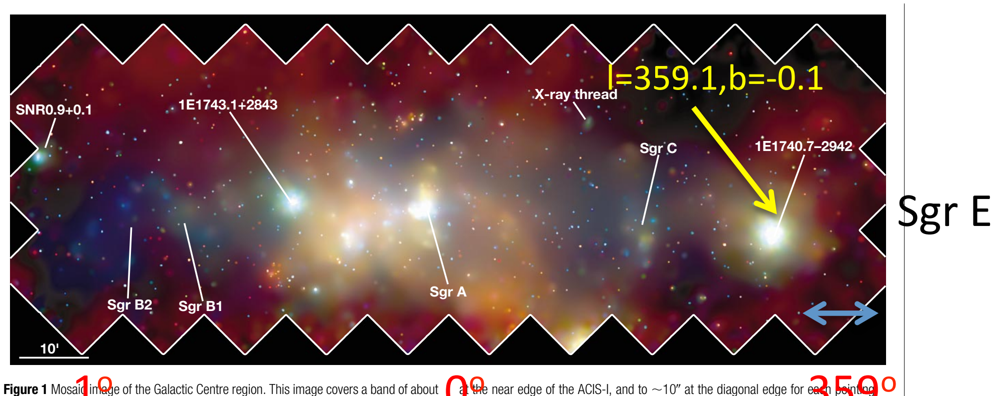

Figure 1 Mosaic image of the Galactic Centre region. This image covers a band of about 2° × 0.8° in Galactic coordinates, and is centred at longitude $l = -0.1°$, latitude $b = 0°$, roughly the location of the Sgr A complex. The three energy bands are 1–3 keV (shown in red), 3–5 keV (green), and 5–8 keV (blue). The data consist of 30 separate pointings, and were acquired during July 2001 with the front-illuminated Advanced CCD Imaging Spectrometer (ACIS-I). The spatial resolution ranges from ~0.5″ on-axis, to ~5″ at the near edge of the ACIS-I, and to ~10″ at the diagonal edge for each pointing. This image is adaptively smoothed with a signal-to-noise ratio of 3. The intensity is plotted logarithmically to emphasize low-surface-brightness features. Standard imaging calibration and exposure correction have been applied, as well as corrections for charge transfer inefficiency effects[5,25].

Summary

- Spectrally resolved [C II] and [N II] far-IR lines provide detailed information about the location, morphology, and physical environment of the dense ionized gas in the CMZ.
- We find n(e)≈ 5 – 25 cm^{-3} at the interface of GMCs in regions about 10 – 20 pc in size
- Mapping the ionized gas throughout the CMZ in spectrally resolved [N II] is difficult because of the weakness of the emission lines.
- GREAT on SOFIA provides a platform to study the electron abundance and ionization in select regions of the CMZ.
- To trace the highly ionized gas throughout the CMZ it will be important to extend the [N II] observations using a survey instrument on balloon borne or orbital platforms.